Acta Crystallographica Section C
Crystal Structure Communications
ISSN 0108-2701

Powder X-ray studies of *meso*-hexamethyl propylene amine oxime (*meso*-HMPAO) in two different phases

Mahmoud Al-Ktaifani and Mwaffak Rukiah*

Department of Chemistry, Atomic Energy Commission, PO Box 6091, Damascus, Syrian Arab Republic
Correspondence e-mail: cscientific@aec.org.sy

Received 8 July 2010
Accepted 9 August 2010
Online 21 August 2010

Two different forms of *meso*-3,3′-[2,2-dimethylpropane-1,3-diylbis(azanediyl)]dibutan-2-one dioxime, commonly called *meso*-hexamethyl propylene amine oxime (HMPAO), $C_{13}H_{28}N_4O_2$, designated α and β, were isolated by fractional crystallization and their crystal structures were determined by powder X-ray diffraction using the direct-space method with the parallel tempering algorithm. The α form was first crystallized from acetonitrile solution, while the β form was obtained by recrystallization of the α phase from diethyl ether. The α form crystallizes in the triclinic system (space group $P\overline{1}$), with one molecule in the asymmetric unit, while the crystal of the β form is monoclinic (space group $P2_1/n$), with one molecule in the asymmetric unit. In both phases, the molecules have similar conformations and *RS*/*EE* geometric isomerism. The crystal packing of the two phases is dominated by intermolecular hydrogen-bonding interactions between the two O—H oxime groups of an individual molecule and the amine N atoms of two different adjacent molecules, which lead to segregation of extended poly(*meso*-HMPAO) one-dimensional chains along the *c* direction. The structures of the two phases are primarily different due to the different orientations of the molecules in the chains.

Comment

It is well known that both diastereomeric forms of hexamethyl propylene amine oxime, *meso*-HMPAO, (I), and D,L-HMPAO, (II), have important radiopharmaceutical applications in nuclear medicine after labelling with ^{99m}Tc (Neirinckx *et al.*, 1987; Sasaki & Senda, 1997; Roth *et al.*, 1992; Jurisson *et al.*, 1986). For example, ^{99m}Tc-D,L-HMPAO has been widely used as a leukocyte labelling agent and for SPECT (single photon emission computed tomography) imaging of regional cerebral blood perfusion (Jurisson *et al.*, 1986).

The most general reported synthetic route to the diastereomeric mixture of HMPAO involves two synthetic procedures (Jurisson *et al.*, 1986; Banerjee *et al.*, 1999), which give a 50:50 diastereomeric mixture of HMPAO, *viz.* *meso*-HMPAO, (I), and D,L-HMPAO, (II), that can be separated by fractional crystallization using different solvents (Banerjee *et al.*, 1999). ^{1}H and ^{13}C{^{1}H} NMR spectroscopic techniques may be utilized to assess the relative amounts of the *meso*-HMPAO and D,L-HMPAO isomers in the diastereomeric mixture and

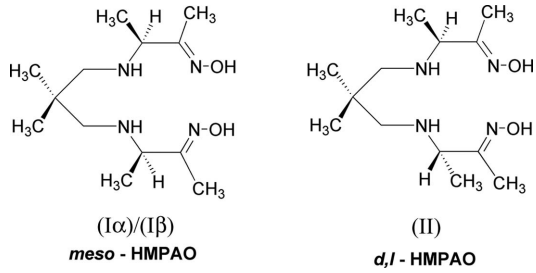

also to identify the purity of each isomer obtained from such a mixture (Feinstein-Jaffe *et al.*, 1989; Babushkina *et al.*, 2002). Although HMPAO has been used as a polydentate ligand to form metal–HMPAO complexes, some of which have been structurally characterized (Suksai *et al.*, 2008), to the best of our knowledge there are no published reports of the molecular structure of free *meso*-HMPAO, (I), or D,L-HMPAO, (II). Since we are currently interested in preparing HMPAO

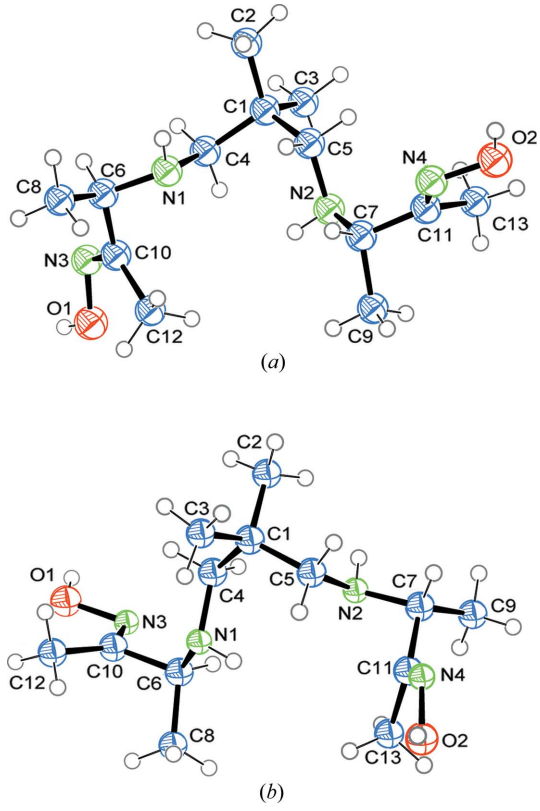

Figure 1
The molecular structures of (*a*) the (Iα) and (*b*) the (Iβ) forms of *meso*-HMPAO, showing the atom-numbering schemes. Displacement ellipsoids are drawn at the 50% probability level and H atoms are shown as small spheres of arbitrary radii.

 doi:10.1107/S0108270110032014

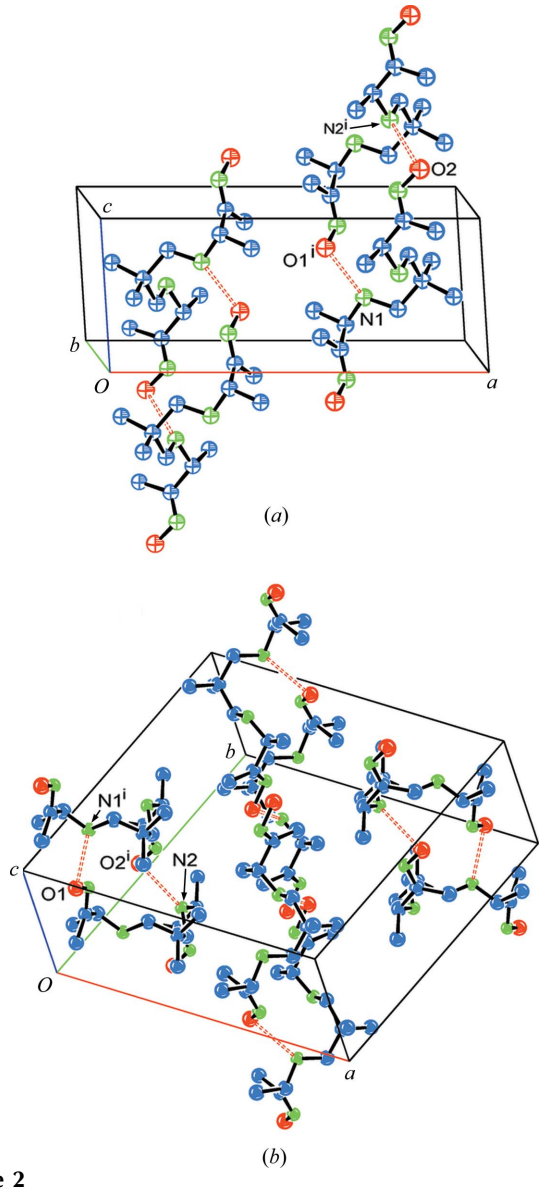

Figure 2
Packing diagrams of (*a*) the (Iα) and (*b*) the (Iβ) forms of *meso*-HMPAO. Oxime–amine O—H···N hydrogen bonds are indicated by dashed lines. H atoms have been omitted for clarity. [Symmetry code: (i) x, y, $z+1$.]

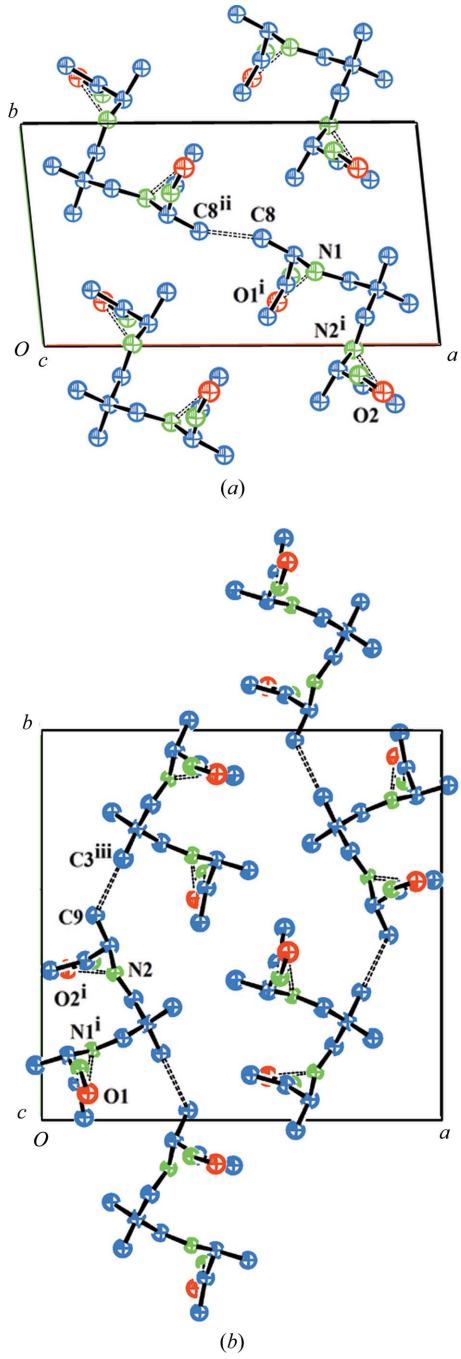

Figure 3
Portions of adjacent molecular chains, viewed along the *c* axis, for (*a*) the (Iα) and (*b*) the (Iβ) forms of *meso*-HMPAO. Hydrogen bonds and short contacts between adjacent molecular chains are indicated by dashed lines. H atoms have been omitted for clarity. [Symmetry codes: (i) x, y, $z+1$; (ii) $-x+1$, $-y+1$, $-z+1$; (iii) $-x+\frac{1}{2}$, $y+\frac{1}{2}$, $-z-\frac{1}{2}$.]

for pharmaceutical applications, we generated the HMPAO mixture, isolated *meso*-HMPAO, and determined the structures of the two crystalline forms that resulted, (Iα) and (Iβ), by powder X-ray diffraction.

Both forms crystallize with one molecule in the asymmetric unit, having almost the same conformations for their corresponding atoms (Fig. 1) and *RS*/*EE* geometric isomerism (Table 1). The crystal system of form (Iα) is triclinic (space group $P\overline{1}$), with two molecules in the unit cell, while (Iβ) is monoclinic (space group $P2_1/n$), with four molecules in the unit cell. In both structures, the molecules are in almost maximally extended forms, with the oxime groups apart. The C—C and N—C bond lengths and bond angles in the {C(HCH$_3$)CNHCH$_2$C(CH$_3$)$_2$CH$_2$NHC(HCH$_3$)C} unit are in their normal ranges (Allen *et al.*, 1987) for single bonds and tetrahedral geometries (Tables 1 and 3). For each individual oxime group in the molecules of (Iα) and (Iβ), the mean distance between the O atom of the C=NOH group and the C atom of the attached CH$_3$ group (*ca* 2.67 Å) lies well within the sum of the van der Waals radii of O and C (3.2 Å; Bondi, 1964). This short distance is likely to be a consequence of the geometrical rigidity introduced by the N=C bond. The molecules of forms (Iα) and (Iβ) display similar bond distances and angles and intermolecular interactions to those in the

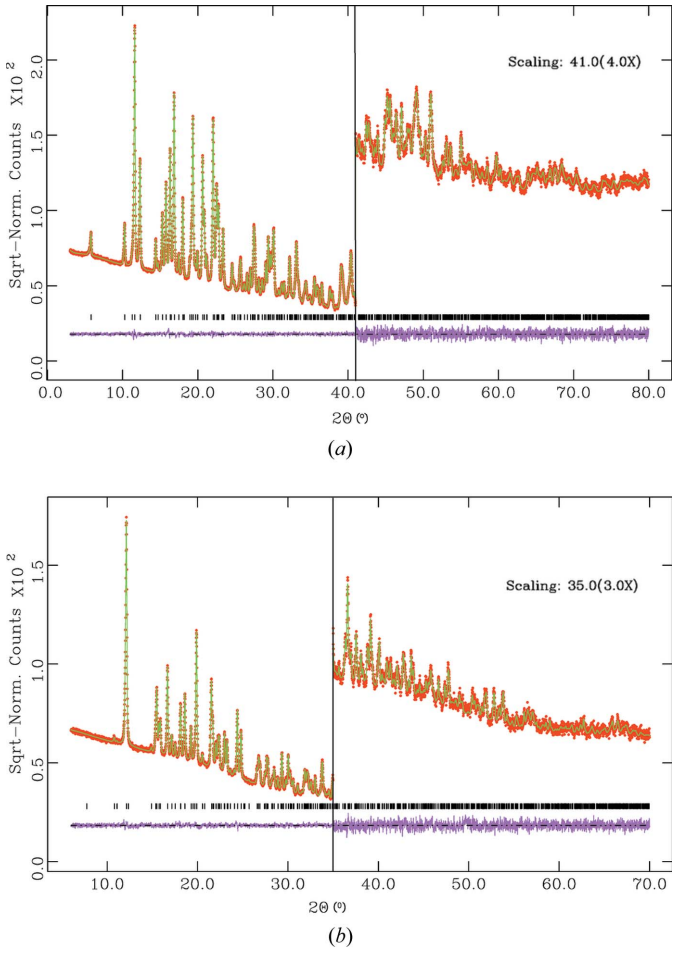

Figure 4
Final observed (points), calculated (line) and difference profiles for Rietveld refinements of (*a*) the α and (*b*) the β forms of *meso*-HMPAO.

closely related compound 3,3′-(trimethylenediamino)bis(3-methyl-2-butanone oxime) ($C_{13}H_{28}N_4O_2$; Hussain *et al.*, 1984). The geometric data for (Iα) and (Iβ) are also comparable with those reported for the recently structurally characterized complex [Ni(*meso*-HMPAO)H]·ClO_4 (Suksai *et al.*, 2008).

In the two phases, a major point of interest is the location of the CH_3, C, N and O centres of each $CH_3C(NOH)$ unit in almost the same plane, as well as the short C—N bond lengths (average 1.30 Å), which readily indicate a $Csp^2{=}Nsp^2$ double bond. The N—O (*ca* 1.40 Å) bond lengths are also characteristic for an oxime group (Allen *et al.*, 1987).

The molecules in both phases are joined by intermolecular O—H···N hydrogen bonds between the two oxime O—H groups of one molecule and the amine N atoms of two different adjacent molecules (Fig. 2, and Tables 2 and 4), leading to one-dimensional chains along the [001] direction. The weak interactions between the chains for both phases involve short contacts between two methyl groups. In (Iα), this short contact is between the C8 methyl group on one chain and a corresponding C8^{ii} [symmetry code: (ii) $-x+1, -y+1, -z+1$] methyl group in an adjacent chain (Fig. 3*a*), while for (Iβ) this short contact is between methyl groups C9 and C3^{iii} [symmetry code: (iii) $-x+\frac{1}{2}, y+\frac{1}{2}, -z-\frac{1}{2}$] in adjacent chains; these C···C distances are 3.579 (4) Å for (Iα) and 3.593 (5) Å for (Iβ) (these distances lie 0.2 Å outside the van der Waals radii sum). In (Iα), the molecules of an individual chain are arranged in opposite orientations to the corresponding ones in an adjacent chain (as required by the inversion symmetry of the $P\overline{1}$ space group), while in (Iβ) the molecules of one chain are rotated by 180° with respect to one another (as required by the twofold screw axis symmetry along the *b* axis of the $P2_1/n$ space group).

As expected, the measured melting points of the two phases are slightly different [424.6 K for (Iα) and 423.1 K for (Iβ)]. Although the difference is small, it may be due to slightly stronger interchain interactions for (Iα) than for (Iβ), which correlates with the marginally shorter interchain contact distances for (Iα).

Experimental

All reactions and manipulations were carried out under an inert atmosphere using a twofold vacuum line and Schlenk techniques. ^{1}H and $^{13}C\{^1H\}$ NMR spectra were recorded in $CDCl_3$ on a Bruker Biospin 400 spectrometer. IR spectra were recorded on a Jasco FT–IR 300E instrument. Microanalysis was performed using a EURO EA analyser. X-ray powder diffraction patterns were obtained on a Stoe Stadi-P diffractometer with monochromatic Cu $K\alpha_1$ radiation (λ = 1.5406 Å) selected using an incident-beam curved-crystal germanium Ge(111) monochromator, using the Stoe transmission geometry (horizontal set-up) with a linear position-sensitive detector (PSD). Melting points were determined by differential thermal analysis measurements on a Netzsch DTA 404 EP instrument. The diastereomeric mixture of HMPAO was prepared and separated by fractional crystallization according to the published method of Banerjee *et al.* (1999). Form (Iα) of HMPAO was first crystallized from acetonitrile solution at room temperature, while form (Iβ) was obtained by recrystallization of (Iα) from diethyl ether at room temperature. The purities of the two *meso*-HMPAO phases were confirmed by multinuclear NMR and IR spectroscopic techniques and microanalysis. Many attempts were made to grow high-quality crystals of *meso*-HMPAO suitable for single-crystal X-ray diffraction study, but without success.

Form (I*α*)

Crystal data

$C_{13}H_{28}N_4O_2$
M_r = 272.39
Triclinic, $P\overline{1}$
a = 15.3159 (3) Å
b = 8.74371 (12) Å
c = 6.21770 (9) Å
α = 81.1652 (10)°
β = 93.4835 (10)°
γ = 96.4282 (8)°
V = 816.80 (2) Å^3
Z = 2
Cu $K\alpha_1$ radiation
λ = 1.5406 Å
μ = 0.61 mm^{-1}
T = 298 K
Flat sheet, 7 × 7 mm

Data collection

Stoe Stadi-P diffractometer
Specimen mounting: drifted powder between two Mylar foils
Data collection mode: transmission
Scan method: step
Absorption correction: cylindrical [*GSAS* absorption/surface roughness correction (Larson & Von Dreele, 2004): function number 4; flat plate in transmission mode, absorption correction term (= $\mu\cdot d$) = 0.16000, correction not refined]
T_{min} = 0.660, T_{max} = 0.669
$2\theta_{min}$ = 2.99°, $2\theta_{max}$ = 79.98°, $2\theta_{step}$ = 0.01°

Table 1
Selected geometric parameters (Å, °) for (Iα).

C4—N1	1.487 (5)	C7—C11	1.498 (5)
N1—C6	1.471 (5)	C10—N3	1.282 (5)
N2—C5	1.492 (4)	C11—N4	1.278 (5)
N2—C7	1.477 (5)	N3—O1	1.407 (5)
C6—C10	1.510 (5)	N4—O2	1.394 (5)
N1—C6—C10	104.8 (5)	C7—C11—C13	118.7 (4)
N2—C7—C11	115.5 (5)	C7—C11—N4	116.2 (5)
C6—C10—C12	118.1 (4)	C13—C11—N4	123.9 (6)
C6—C10—N3	115.5 (5)	C10—N3—O1	112.3 (7)
C12—C10—N3	125.2 (6)	C11—N4—O2	109.7 (6)
C6—N1—C4—C1	164.5 (3)	O2—N4—C11—C13	−14.5 (10)
C4—N1—C6—C8	−167.9 (3)	C8—C6—C10—C12	−61.1 (7)
C7—N2—C5—C1	−170.9 (3)	N1—C6—C10—N3	−132.6 (7)
C5—N2—C7—C9	170.2 (3)	C9—C7—C11—C13	71.3 (6)
O1—N3—C10—C12	−1.2 (11)	N2—C7—C11—N4	120.7 (6)

Table 2
Hydrogen-bond geometry (Å, °) for (Iα).

D—H···A	D—H	H···A	D···A	D—H···A
O1—H1O···N1^{i}	0.82	2.19	2.811 (8)	133
O2—H2O···N2^{ii}	0.82	2.17	2.834 (7)	138

Symmetry codes: (i) $x, y, z-1$; (ii) $x, y, z+1$.

Table 3
Selected geometric parameters (Å, °) for (Iβ).

C4—N1	1.462 (4)	C7—C11	1.530 (5)
C5—N2	1.464 (4)	C10—N3	1.269 (5)
N1—C6	1.463 (5)	C11—N4	1.287 (5)
N2—C7	1.462 (5)	N3—O1	1.411 (5)
C6—C10	1.537 (5)	N4—O2	1.400 (5)
N1—C6—C10	112.9 (5)	C7—C11—C13	123.2 (4)
N2—C7—C11	102.9 (5)	C7—C11—N4	120.7 (6)
C6—C10—C12	121.0 (4)	C13—C11—N4	115.5 (6)
C6—C10—N3	104.0 (5)	C10—N3—O1	104.5 (7)
C12—C10—N3	134.9 (6)	C11—N4—O2	119.0 (7)
C6—N1—C4—C1	−165.5 (4)	O2—N4—C11—C13	3.4 (13)
C4—N1—C6—C8	174.5 (3)	C8—C6—C10—C12	61.4 (7)
C7—N2—C5—C1	166.1 (4)	N1—C6—C10—N3	119.3 (7)
C5—N2—C7—C9	−170.0 (4)	C9—C7—C11—C13	−56.9 (8)
O1—N3—C10—C12	−5.3 (14)	N2—C7—C11—N4	−122.4 (9)

Table 4
Hydrogen-bond geometry (Å, °) for (Iβ).

D—H···A	D—H	H···A	D···A	D—H···A
O1—H1O···N1^{i}	0.82	2.00	2.764 (7)	154
O2—H2O···N2^{ii}	0.82	2.10	2.835 (7)	150

Symmetry codes: (i) $x, y, z+1$; (ii) $x, y, z-1$.

Refinement

R_p = 0.017
R_{wp} = 0.023
R_{exp} = 0.019
$R(F^2)$ = 0.01476
χ^2 = 1.416
7700 data points
224 parameters
104 restraints
H-atom parameters constrained

Form (Iβ)

Crystal data

$C_{13}H_{28}N_4O_2$
M_r = 272.39
Monoclinic, $P2_1/n$
a = 16.4453 (4) Å
b = 15.9587 (3) Å
c = 6.20073 (11) Å
β = 94.7097 (13)°
V = 1621.86 (7) Å^3
Z = 4
Cu $K\alpha_1$ radiation
λ = 1.5406 Å
μ = 0.61 mm^{-1}
T = 298 K
Flat sheet, 7 × 7 mm

Data collection

Stoe Stadi-P diffractometer
Specimen mounting: drifted powder between two Mylar foils
Data collection mode: transmission
Scan method: step
Absorption correction: cylindrical [*GSAS* absorption/surface roughness correction (Larson & Von Dreele, 2004): function number 4; flat plate in transmission mode, absorption correction term (= $\mu \cdot d$) = 0.0434000, correction not refined]
T_{min} = 0.893, T_{max} = 0.894
$2\theta_{min}$ = 5.97°, $2\theta_{max}$ = 69.96°, $2\theta_{step}$ = 0.01°

Refinement

R_p = 0.020
R_{wp} = 0.027
R_{exp} = 0.024
$R(F^2)$ = 0.03684
χ^2 = 1.346
6400 data points
160 parameters
104 restraints
H-atom parameters constrained

The powder of (Iα) or (Iβ) was ground, placed between two foils of Mylar and fixed in the sample holder with a mask of suitable internal diameter (0.7 mm). The pattern of the α form was scanned over the angular range 3–80° (2θ) with a step width of the PSD of 0.1° (2θ) and a counting time of 60 s per step, while the pattern of the β form was scanned over the angular range 5–70° (2θ) with a step width of the PSD of 0.5° (2θ) and a counting time of 420 s per step. Pattern indexing was performed using the *DICVOL4.0* program (Boultif & Louër, 2004) with default options. Confidence factors were $M(20)$ = 34.1 and $F(20)$ = 96.4 for the α form, and $M(20)$ = 32.4 and $F(20)$ = 85.4 for the β form. The space groups were obtained using the program *CHECK-CELL*, interfaced by *WINPLOTR* (Roisnel & Rodriguez-Carvajal, 2001). The unreduced triclinic cell for (Iα) was used to make the c axis the common axis for the molecular chains in the two phases.

Direct methods were initially employed to determine the crystal structures using the program *EXPO2004* (Altomare *et al.*, 1999), but they were not successful. Starting models for the two forms were obtained using the direct-space method with the parallel tempering algorithm in the program *FOX* (Favre-Nicolin & Černý, 2002). One molecule of *meso*-HMPAO for both phases was introduced randomly with the possibility to translate, to rotate around its centre of mass and to modify its ten torsion angles. The degree of freedom for the molecular replacement for the two forms is 16. In order to accelerate the process during the parallel tempering calculation, the powder patterns were truncated to 36° (Cu $K\alpha_1$) and the H atoms were not introduced. This method yielded a suitable model with agreement factors of R_p = 0.0776 for (Iα) and R_p = 0.0459 for (Iβ).

The two models thus obtained were used as starting points for Rietveld refinements in the program *GSAS* (Larson & Von Dreele, 2004), interfaced by *EXPGUI* (Toby, 2001). The coordinates of the 19 non-H atoms were refined with soft constraints on bond lengths. The

profile function used was a pseudo-Voigt function convoluted with an axial divergence asymmetry function (Finger *et al.*, 1994), and with *S*/*L* and *D*/*L* both fixed at 0.0225.

An isotropic displacement parameter was introduced and refined for each type of atom. Intensities were corrected for absorption effects with a $\mu \cdot d$ value of 0.1600 for (Iα) and 0.0434 for (Iβ) (μ is the absorption coefficient and d is the sample thickness). Before the final refinement, H atoms of the CH, CH_2 and CH_3 groups were introduced from geometric arguments and refined with constraints to the riding atoms (0.99 Å for CH, 0.98 Å for CH_2 and 0.97 Å for CH_3). The H atoms of the hydroxy and amine groups were localized by difference Fourier syntheses and refined with constraints on bond lengths (0.82 Å for OH and 0.87 Å for NH) and angles. The background was refined using a shifted Chebyshev polynomial with 15 coefficients, whereas the preferred orientation was modelled using the generalized spherical-harmonics description (Von Dreele, 1997).

Final agreement factors are provided in the experimental tables. Fig. 4 shows the experimental X-ray patterns, together with the calculated patterns and difference curves from the final Rietveld refinements for both forms.

For both compounds, data collection: *WINXPOW* (Stoe & Cie, 1999); cell refinement: *GSAS* (Larson & Von Dreele, 2004); data reduction: *WINXPOW*; program(s) used to solve structure: *FOX* (Favre-Nicolin & Černý, 2002); program(s) used to refine structure: *GSAS* (Larson & Von Dreele, 2004); molecular graphics: *ORTEP-3* (Farrugia, 1997); software used to prepare material for publication: *publCIF* (Westrip, 2010).

The authors thank Professor I. Othman, Director General, and Professor T. Yassine, Head of Chemistry Department, for their support and encouragement to achieve this work. We also thank Chem. M. A. Nakawa for his assistance with some of the laboratory work.

Supplementary data for this paper are available from the IUCr electronic archives (Reference: SQ3256). Services for accessing these data are described at the back of the journal.

References

Allen, F. H., Kennard, O., Watson, D. G., Brammer, L., Orpen, A. G. & Taylor, R. (1987). *J. Chem. Soc. Perkin Trans. 2*, pp. S1–19.
Altomare, A., Burla, M. C., Camalli, M., Carrozzini, B., Cascarano, G. L., Giacovazzo, C., Guagliardi, A., Moliterni, A. G. G., Polidori, G. & Rizzi, R. (1999). *J. Appl. Cryst.* **32**, 339–340.
Babushkina, T. A., Klimova, T. P., Sviridov, B. D. & Antonyuk, A. V. (2002). *Russ. J. Coord. Chem.* **28**, 71–74.
Banerjee, S., Samuel, G., Kothari, K., Sarma, H. D. & Pillai, M. R. A. (1999). *Nucl. Med. Biol.* **26**, 327–338.
Bondi, A. J. (1964). *J. Chem. Phys.* **68**, 441–451.
Boultif, A. & Louër, D. (2004). *J. Appl. Cryst.* **37**, 724–731.
Farrugia, L. J. (1997). *J. Appl. Cryst.* **30**, 565.
Favre-Nicolin, V. & Černý, R. (2002). *J. Appl. Cryst.* **35**, 734–743.
Feinstein-Jaffe, I., Boazi, M. & Tor, Y. (1989). *J. Nucl. Med.* **30**, 106–109.
Finger, L. W., Cox, D. E. & Jephcoat, A. P. (1994). *J. Appl. Cryst.* **27**, 892–900.
Hussain, M. S., Mazhar-ul-Haque & Ahmed, J. (1984). *Acta Cryst.* C**40**, 813–816.
Jurisson, S., Schlemper, E. O., Troutner, D. E., Canning, L. R., Nowotnik, D. P. & Neirnckx, R. D. (1986). *Inorg. Chem.* **25**, 543–549.
Larson, A. C. & Von Dreele, R. B. (2004). *GSAS*. Report LAUR 86-748. Los Alamos National Laboratory, New Mexico, USA.
Neirinckx, R. D., Canning, L. R., Piper, I. M., Nowotnik, D. P., Pickett, R. D., Holems, R. A., Volkert, W. A., Forster, A. M., Weisnwer, P. S., Marriott, J. A. & Chaplin, S. B. (1987). *J. Nucl. Med.* **28**, 191–202.
Roisnel, T. & Rodriguez-Carvajal, J. (2001). *Mater. Sci. Forum*, **378–381**, 118–123.
Roth, C. A., Hoffman, T. J., Corlija, M., Volkert, W. A. & Homles, R. A. (1992). *Nucl. Med. Biol.* **19**, 783–790.
Sasaki, T. & Senda, M. (1997). *J. Nucl. Med.* **38**, 1125–1129.
Stoe & Cie (1999). *WINXPOW*. Stoe & Cie, Darmstadt, Germany.
Suksai, C., Pakawatchai, C. & Thipyapong, K. (2008). *Polyhedron*, **27**, 759–764.
Toby, B. H. (2001). *J. Appl. Cryst.* **34**, 210–213.
Von Dreele, R. B. (1997). *J. Appl. Cryst.* **30**, 517–525.
Westrip, S. P. (2010). *J. Appl. Cryst.* **43**, 920–925.